EUROPEAN ORGANIZATION FOR NUCLEAR RESEARCH

CERN/EP 85-165
8 October 1985

A MEASUREMENT OF THE TOTAL CHARM CROSS SECTION IN 200 AND 360 GeV/c pN INTERACTIONS USING A HOLOGRAPHIC BUBBLE CHAMBER

O. Erriquez, M. Calicchio, M.T. Muciaccia, S. Natali, S. Nuzzo[1] and F. Ruggieri[1]
Universita di Bari, Bari, Italy

M. Barth[2], H. Cobbaert[3], D. Geiregat[3], R. Roosen[4] and S.P.K. Tavernier[4]
Inter-University Institute for High Energies, Brussels, Belgium

H. Drevermann, K. Geissler, A. Hervé, E. Johansson[5], P. Lecoq, N. Minaev and P. Olivier[6]
CERN, European Organization for Nuclear Research, Geneva, Switzerland

J.H. Bartley, F.W. Bullock, M. Coupland, R. Cranfield, B.G. Duff†, M.J. Esten, I. Gjerpe, F.F. Heymann, P.R. Hobson, D.C. Imrie[7], G.J. Lush and O.R. Williams[8]
Physics and Astronomy Department, University College, London, U.K.

J.L. Bailly, J.F. Baland, F. Grard, V.P. Henri and J. Kesteman
Université de l'Etat à Mons, Belgium

M. Boratav, M.C. Touboul and A.M. Touchard
LPNHE, Université de Paris VI et Paris VII, Paris, France

K. Arnold, and G. Maurer
Centre de Recherches Nucléaires et Université Louis Pasteur, Strasbourg, France

J. Hrubec, G. Neuhofer and A. Taurok
Institut für Hochenergiephysik der Osterreichischen Akademie der Wissenschaften, Wien, Austria

1 INFN Bari, Italy
2 Chercheur agréé FNRS, Belgium
3 Vorser IIKW, Belgium
4 Bevoegdverklaard Navorser, NFWO, Belgium
5 Now at the University of Stockholm, Sweden
6 Now at Physics Department, Yale University, New Haven, USA
7 Now at Physics Department, Brunel University, Uxbridge, U.K.
8 Now at Imperial College, London, U.K.
† We very much regret the death of our respected colleage

Submitted to Physica Scripta

EP/2722P/HD/sb

ABSTRACT

We present results from the first holographic bubble chamber experiment. Using topological information on the events observed in the heavy liquid bubble chamber HOBC, we have determined a total charm pair production cross section of $(24.6^{+12.0}_{-8.3})$ μb and $(3.9^{+2.5}_{-1.9})$ μb in 360 GeV/c and 200 GeV/c proton-nucleon interactions respectively. For these estimates we assumed a linear dependance of the charm cross section on the atomic number A.

Due to the short lifetime, visual detection of charmed particles requires very high spatial resolution. Particularly in hadronic interactions where the charm cross section is of the order of 10^{-3} of the total cross section, a direct observation of the charm decay is at a premium to obtain a clean sample of events. Holographic image recording has been used to improve the resolution of bubble chambers. The main advantage of holography is the possibility to obtain high resolution and a large depth of field simultaneously. With a conventional optical system the depth of field and the resolution are related, and high resolution can only be obtained at the expense of the depth of field. The pioneering work on the hologhaphic photography of bubble chamber tracks was performed with the heavy liquid bubble chamber BIBC [1].

Below we report results on the total charm cross section in 200 and 360 GeV/c proton-nucleon interactions from the hologhaphic bubble chamber experiment NA25 [2]. In this experiment the charm cross section is measured for the first time at different beam energies with the same apparatus. Particularly at lower energy there is considerable confusion about the value of the charm cross section. Some experiments [3, 4] have reported results which imply a large (> 10 μb) cross section at incident momenta as low as 50 GeV/c, while other experiments [5, 6, 7] provide measurements or upper limits which suggest a cross section well below 10 μb.

The data were taken with a positive, unseparated beam at the CERN SPS accelerator. At 360 GeV/c the beam contained only protons, while at 200 GeV/c it contained 76.4% protons, 21% pions and 2.6% kaons. The protons and the pions were tagged with two beam Cherenkov counters (CEDAR counters). Our results correspond to data with incoming protons only.

The main components of the experimental arrangement are the holographic bubble chamber (HOBC) and a muon detector. The muon detector was composed of a 2 m long block of iron with a tungsten core, followed by an instrumented part which consisted of a sandwich of iron blocks, proportional wire chambers and scintillator hodoscopes (fig. 1). The muon trigger required at least one hit in each of the two H1 scintillator hodoscopes. Particles emitted at less than 54 mrad from the beam

direction had to penetrate 6.5 cm of copper 200 cm of tungsten and 40 cm of iron. Particles emitted at larger angles had to penetrate ~ 240 cm of iron to reach the hodoscope. This corresponds to a momentum cut off for the muons of 5.8 and 3.1 GeV/c respectively. Muons emitted at angles larger than about 100 mrad would miss the proportional chambers W1 and were rejected in the off line analysis. The muon trigger is essential since it improves the signal to background ratio by a factor of ~ 20.

The target was a small, heavy liquid, rapid cycling bubble chamber designed for in-line holography [8, 9]. A fast kicker magnet upstream of the primary target in the beam line was used to suppress the beam during 2.5 ms before and after a 200 μs window in the middle of the expansion cycle. The chamber was filled with Freon C_3F_8 and the visible volume was 5 X 6.2 X 10 cm^3. The data were taken with a repetition rate of 10 Hz, the bubble density was 95 cm^{-1} and the bubble diameter was 12 μm FWHM. As the three dimensional properties of a hologram make it possible to measure all three space coordinates in one image, only one hologram was recorded per event. The holograms were recorded with a two stage excimer dye laser producing 10 ns pulses at a wavelength of 514 nm. This wavelength was chosen to match the green line of the argon ion lasers used in the replay systems.

The event trigger demanded one incident particle, an interaction in HOBC and at least one muon in the muon detector. An interaction in HOBC was signed by a pulse height exceeding 2.3 times that produced by a minimum ionising particle in each of the four S3 scintillators. With this trigger a total of 23000 and 17000 holograms were recorded at 360 and 200 GeV/c respectively.

In the off line analysis the events were required to have a reconstructed muon track in the wire chambers W1 downstream of the dump, and an interaction in the fiducial volume of the bubble chamber. About 27% of the triggers fulfilled these requirements. Each hologram contains typically 70 incoming beam tracks and 5 interactions. With conventional photography such pictures would be too complex to analyse. The proportional chambers B1 and B2 (fig. 1) consist of two orthogonal planes of 1 mm pitch and were used to identify the beam track corresponding to

the trigger. An interaction was retained for further analysis only if it was situated at least 15 mm upstream of the visible end of the chamber, and if the incoming beam track had a visible length in the bubble chamber of at least two mm. A tolal of 12% of the events was rejected because of poor picture quality or ambiguous beam track.

Two independent scans were made and the differences were checked by a physicist. Any activity in a 2.8 mm wide band forward from the primary vertex was recorded. A decay candidate was required to have correct multiplicity (neutral decays must have even and charged decays odd multiplicity) and no heavily ionising or backward going track. In addition no decay track sould show evidence for multiple scattering. This last requirement removes less than 3% of the genuine charm decays but most of the interactions, gamma conversions or delta electrons.

For each event with secondary activity the primary and secondary vertices were accurately measured. For each decay candidate a point on each secondary decay track was also measured. The measurement accuracy in the plane perpendicular to the optical axis is 6 μm in space (rms). Position measurements along the optical axis were done by focussing on a bubble and have an accuracy of 120 μm on isolated tracks. The presence of other tracks in the vicinity of the one being measured can however degrade this resolution by a factor two or more. A total of 4117 and 2208 primary interactions were retained for final analysis at 360 and 200 GeV/c respectively.

In this experiment the charm signal is extracted using only the topological and geometrical information on the charm decay candidates. To reduce the background we required the transverse decay distance, the impact parameter and the decay angles to satisfy the cuts listed in table 1. The transverse decay distance and the impact parameter are defined in fig. 2. The parameters are of the order of the proper decay length of the decaying particle (~ CT) and thus of the order of a few hundred microns for charm particles. Because of the limited accuracy of the depth measurement the cuts are always imposed on quantities projected on the film plane. The cuts on the transverse decay distance and the impact parameter remove only a few percent of the genuine charm decays. However a minimum kink angle

for charged one prong decays and a minimum opening angle for other decays is necessary to reduce the contamination by electrons where a small amount of multiple scattering simulates a one prong decay, or by gamma conversions simulating a multi prong decay. These cuts remove a significant fraction of the charm decays as can be seen in table 1. Table 2 gives the total number of charm candidates satisfying these cuts.

We have used the events with two charm candidates to determine the charm pair production cross section. An example of such an event is shown on fig. 3. The background in the double charm decays due to accidental occurrence of two unrelated background charm candidates at the same primary vertex has been estimated using the total number of charm candidates and assuming that they are all background. At 360 GeV/c we observe 15 events with two charm candidates with an estimated background of 1.9 events. At 200 GeV/c we observe 8 events with a background of 2.0. The method to estimate the background was verified on a sample that did not contain charm. The correct number of double decays was predicted (see table 3). We conclude that there is a clear signal for charm decay both at 360 and at 200 GeV/c.

To calculate the cross sections we need to evaluate the trigger acceptance, the corrections due to the charm decay candidate cuts and the detection efficiency for charm decays in the scanning of the holograms. This was done with a detailed Monte Carlo simulation. The trigger acceptance is 9.4% and 7.9% at 360 and 200 GeV/c respectively. This contains the geometrical acceptance of the muon detector (47% and 40% at 360 and 200 GeV/c respectively) and the semileptonic branching ratios: $D^{\pm}$: 17.2%, D^{o} or $F^{\pm}$: 6%, and Λ_c: 4.5%. We further assumed that all charm is produced either as a meson-antimeson pair, or as a Λ_c-antimeson pair. The charm meson mixture was 39% $D^{\pm}$, 53% D^{o} and 8% of $F^{\pm}$. The weight factor to correct for the charm decay candidate selection cuts is 1.28 and 1.19 per decay at 360 and 200 GeV/c respectively. The visual detection efficiency for short decay lengths is determined from a comparison of the decay length distribution for all charm decays occuring in pairs with the Monte Carlo simulation. This was done by parametrising the visual detection efficiency as $V = 1 - \exp(-\beta \times L)$, in a maximum likelihood fit to the two aforementioned distributions. From this fit the average detection

efficiency for charm decays was estimated at 0.52 ± 0.14 at 360 GeV/c and at $0.94^{+0.06}_{-0.29}$ at 200 Gev/c. The larger detection efficiency at 200 GeV/c is due both to the improved picture quality at the end of the run when the 200 GeV/c data were taken, and to the reduction in event complexity at lower energy. The scanning efficiency at large decay lengths (> 10 mm) is determined to be (90 ± 3)% from a comparison of the two independent scans.

The resulting total charm pair production cross sections per nucleon are (22 ± 11)μb and $(3.9^{+2.5}_{-1.9})$μb in 360 and 200 GeV/c proton nucleon interactions respectively. We have assumed a linear dependence of the charm cross section on the atomic number A, and a negligible contribution of Λ_c production to the total cross section. With a 20% $\Lambda_c\bar{D}$ production the cross section estimated will increase by 17% at 360 GeV/c and by 8% at 200 GeV/c.

An independant determination of the charm cross section at 360 GeV/c was obtained from a study of the decay length distribution for the events with only one charm decay candidate. Using the charm candidate selection cuts described above excluding the impact parameter cut, we obtain a sample of 341 charm decay candidates. The impact parameter cut would introduce a bias in the length distribution which it would be difficult to correct for. The transverse decay length cut and the effect of the finite chamber length can be allowed for by proper weighting of the events. After a correction for the loss at small decay lengths with the visibility as a function of length determined in the charm pair production analysis above, the background events have a flat decay length distribution. The correctness of the procedure was checked with secondary interactions. Fig. 4 shows the length distribution of the charm particles after application of the procedure described. The flat background at large distances is clearly visible. This background is extrapolated to zero decay length and the excess in the region between zero and 18 mm is interpreted as due to charm. The resulting charm pair production cross section is (29^{+24}_{-13})μb. Combining this with the result from the previous analysis gives $(24.6^{+12.0}_{-8.3})$μb.

Several experiments have reported charm cross sections in proton-nucleon interactions for incident momenta in the range of 350-400 GeV/c. All recent results are compatible with a total cross section of ~ 20 μb if an A^{α} with $\alpha = 1$ dependence of the cross section on the atomic number is assumed. Comparing our result with the result from NA16 [10] which used a hydrogen target $(15.5^{+8.2}_{-4.6})$μb gives $\alpha = 1.16^{+0.20}_{-0.22}$.

The strong energy dependence of the cross section found here is in agreement with most model calculations [11].

Acknowledgements

This experiment, which used a novel technique, resulted in difficult working conditions for our scanning teams. We should like to take this opportunity of thanking them for the painstaking efforts throughout the course of this work.

REFERENCES

[1] M. Dykes et al., Nucl. Instr. and Meth. 179 (1981) 487.

[2] J.F. Baland et al., CERN/SPSC/80-120.

[3] A.N. Aleev et al., Sov. J. Nucl. Phys. 37 (1983) 877;
A.N. Aleev et al., Z. Phys. C, Particles and Fields, 23 (1984) 333;
A.N. Aleev et al., The inclusive production of the charm baryon Λ_C in neutron carbon interactions, Contributed paper to the 22th International Conference on High Energy Physics, Leipzig, July 1984.

[4] S.F: Biagi et al., Phys. Lett. 122B (1983) 455;
S.F. Biagi et al., Phys. Lett. 150B (1985) 230.

[5] A.E. Asratyan et al., Phys. Lett. 79B (1978) 497.

[6] Balley et al., Nucl. Phys. 239B (1984) 15.

[7] Theses by P.L. Mcbride and Liang Tzeng, Yale University 1984.

[8] A. Hervé et al., Nucl. Instr. and Meth. 202 (1982) 417.

[9] J.L. Benichou et al., Nucl. Instr. and Meth. 214 (1983) 245.

[10] M. Aguilar-Benitez et al., Phys. Lett. 135B (1984) 237.

[11] S. Tavernier, Hadroproduction of charm, Review talk at the 22th International Conference on High Energy Physics, Leipzig, July 1984 161.

TABLE CAPTIONS

Table 1 Geometrical cuts which define a charm decay candidate. The corresponding selection efficiencies for genuine charm decays at 360 GeV/c are also given. The cuts refer to quantities projected on the plane perpendicular to the optical axis. At 200 GeV/c the numbers are very similar. The average selection efficiency is 78% and 84% at 360 and 200 GrV/c respectively.

Table 2 Total number of primary vertices analysed and number of events with one or two charm decay candidates at the same vertex.

Table 3 Number of events with two or more secondary activities as predicted under the assumption of uncorrelated production and detection efficiencies, compared with the observed number for decay categories containing little or no charm (360 GeV/c data).

TABLE 1

Decay topology	Max. L_T(μm)	Max. L_{imp}(μm)	Min opening or kink angle (mrad)	Selection efficiency %
1 prong	500	1000	10	63
3 prong	500	2000	5	97
2 prong	300	1000	10	81
4 prong	300	1000	5	99

Table 2

Momentum (GeV/c)	No. of primary vertices	No. of singles	No. of doubles
200	2208	93	8
360	4117	159	15

Table 3

Category	No. of doubles observed	No. of doubles predicted
Secondary interactions	148	162
Decay topologies without the cuts of table 1	317	279

FIGURE CAPTIONS

Fig. 1 General layout of the experiment. B1 and B2 are beam defining proportional wire chambers, S1-S3 are scintillation counters, H1-H3 are scintillation hodoscopes and W1-W7 are proportional wire chambers.

Fig. 2 Definition of the geometrical quantities used to select charm decays.

Fig. 3 Example of a double charm decay. The picture is a computer generated perspective view. Angles and distances are non-linearly distorted. The event contains a one prong and a three prong decay at 8.9 and 12.1 mm from the primary vertex. The one prong kink angle is 2.7°, and the three prong opening angle is 1.1°.

Fig. 4 Weighted length distribution for charged and neutral charm candidates.

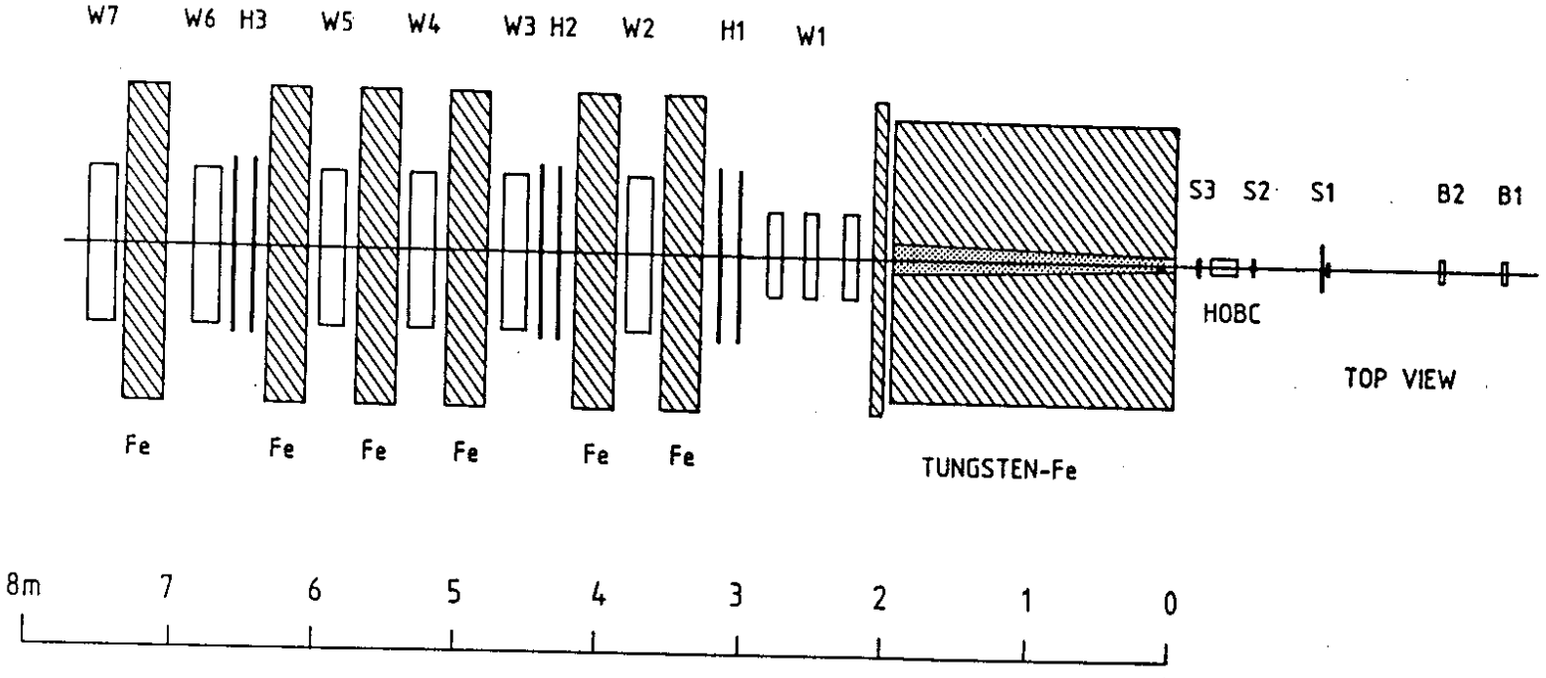
W7
W6
H3
W5
W4
W3
H2
W2
H1
W1
S3
S2
S1
B2
B1
HOBC
TOP VIEW
Fe
Fe
Fe
Fe
Fe
Fe
TUNGSTEN-Fe
8m
7
6
5
4
3
2
1
0

Fig. 1

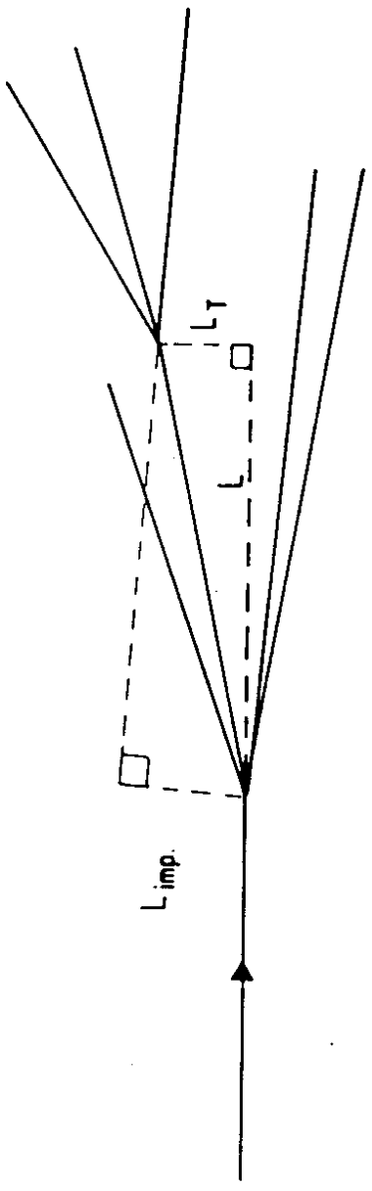

Fig. 2

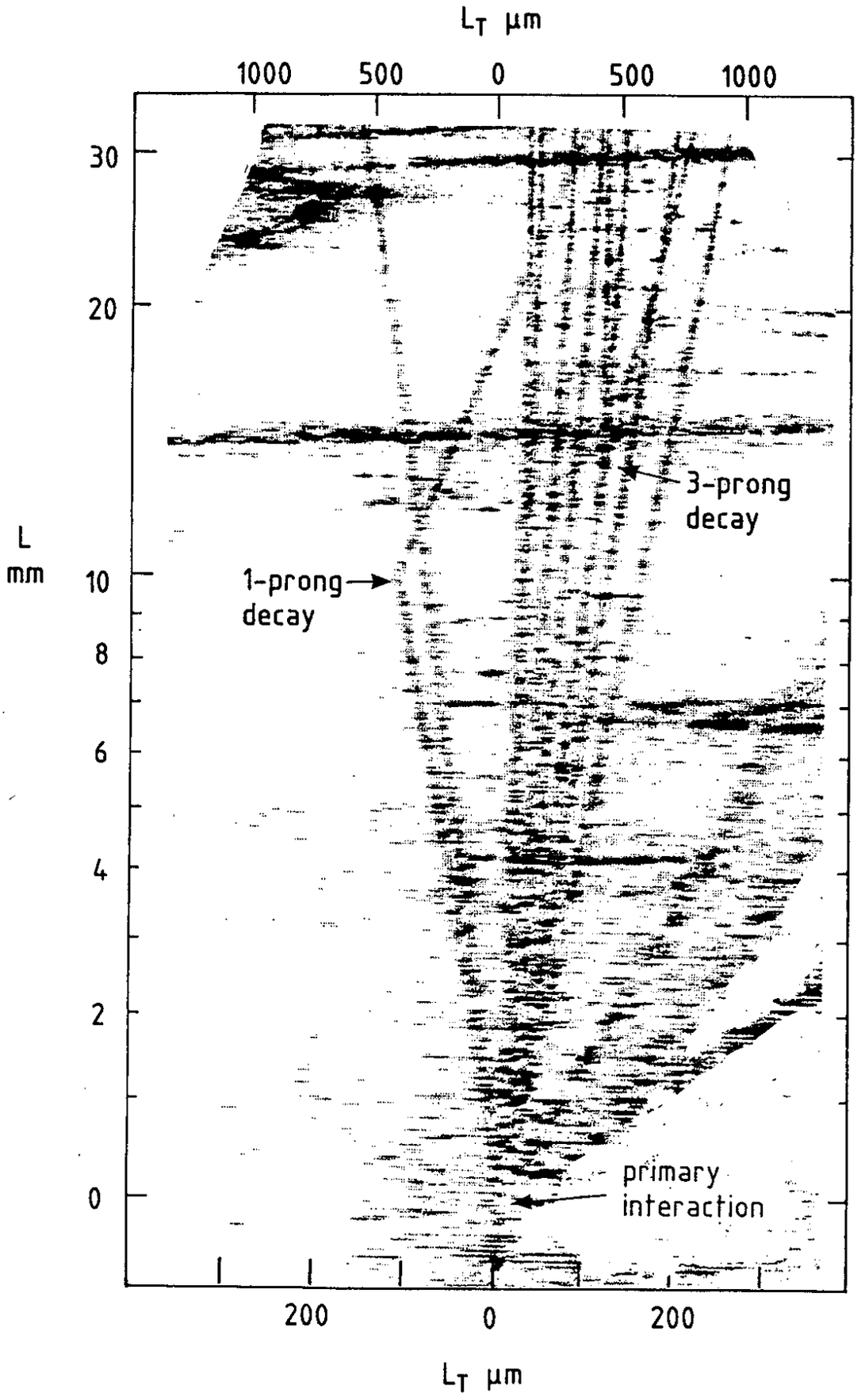
L_T μm
1000
500
0
500
1000
30
20
10
8
6
4
2
0
L
mm
3-prong
decay
1-prong
decay
primary
interaction
200
0
200
L_T μm

Fig. 3

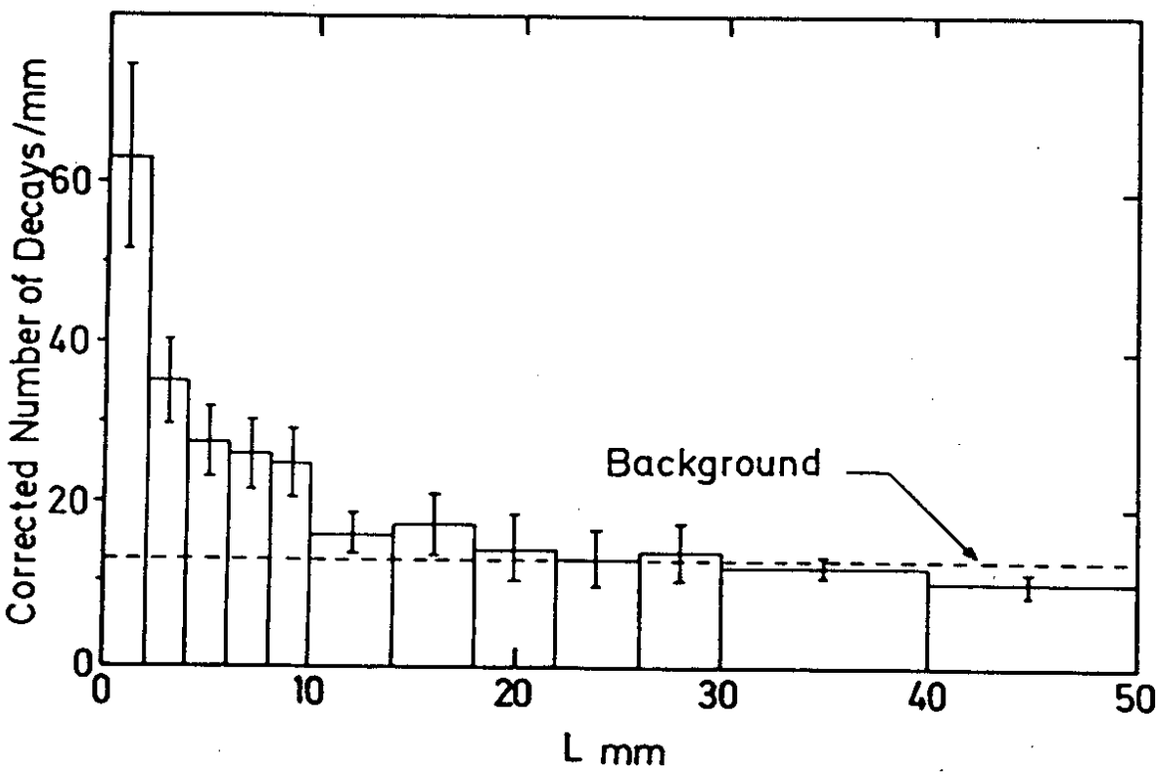
Corrected Number of Decays/mm
60
40
20
0
0
10
20
30
40
50
L mm
Background

Fig. 4